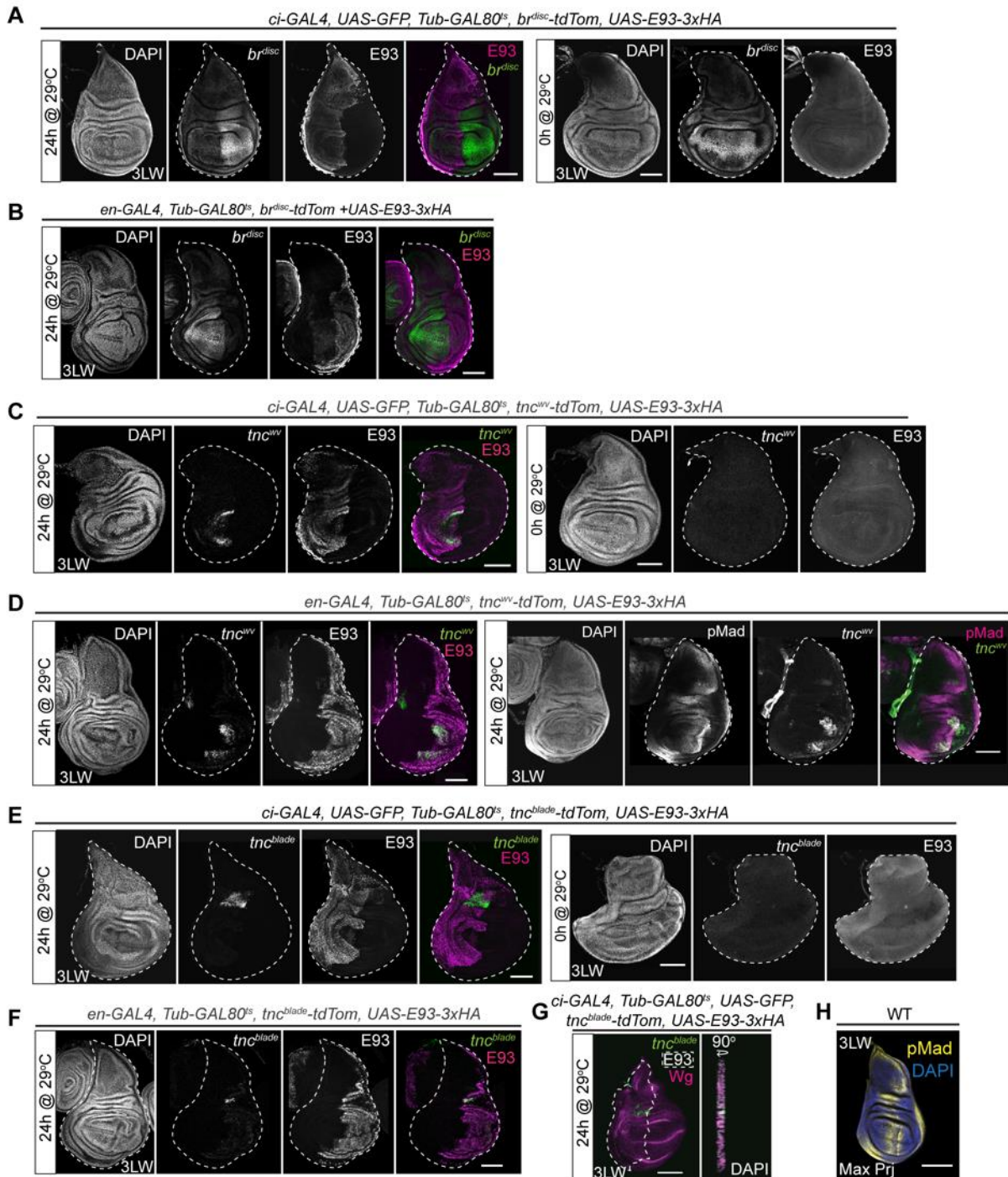
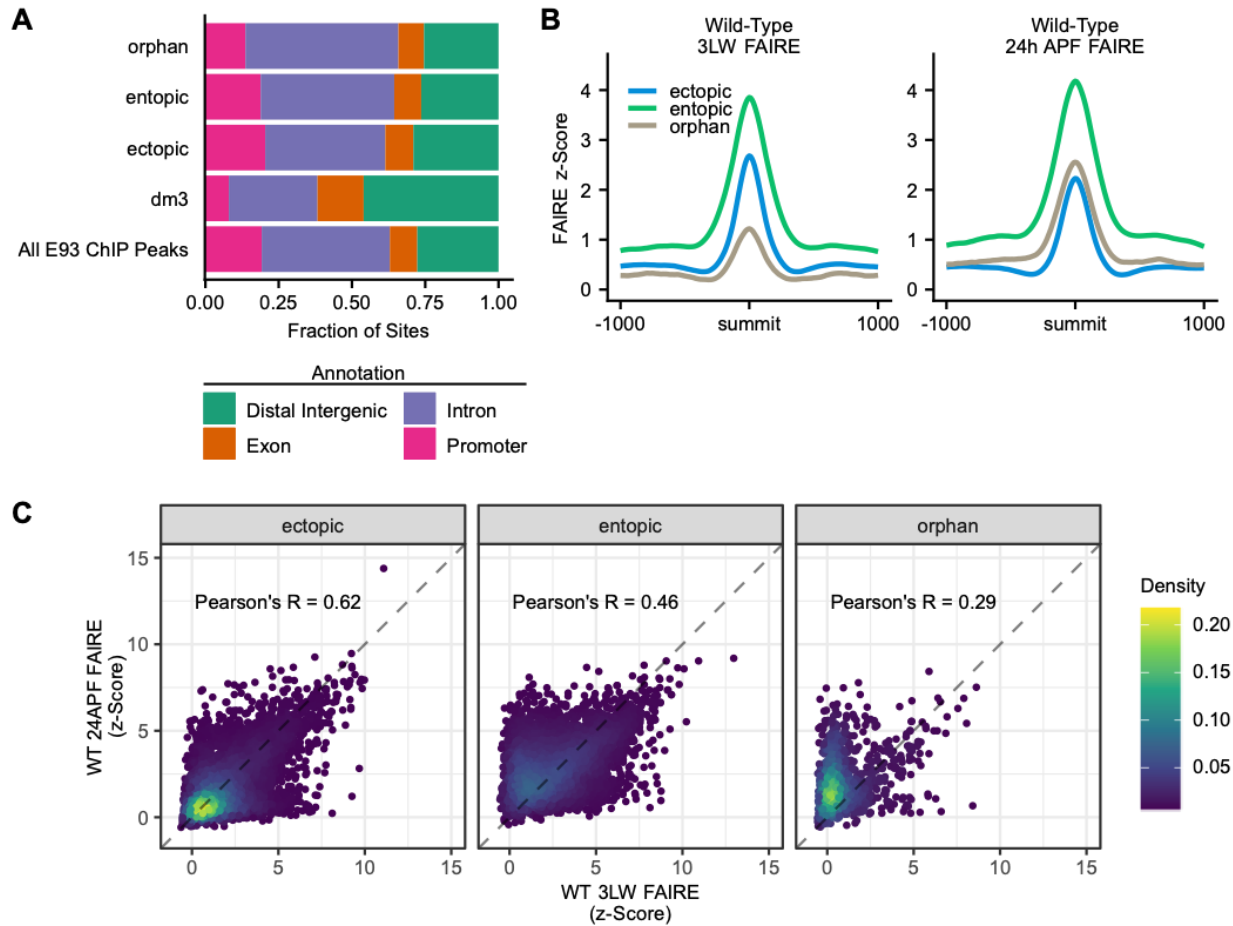


**Fig. S1. Ectopic E93 expression system leads to two-fold higher levels of E93 relative to endogenous expression.** (A) Experimental details of *ci-GAL4/GAL80<sup>ts</sup>* control of the *UAS-E93-3xHA* transgene. Crosses were raised at room temperature (~22°C), at which temperature *GAL80<sup>ts</sup>* is stable and can repress *GAL4* activity, until mid-third instar (144h-168h). They were then switched to 29°C, at which temperature *GAL80<sup>ts</sup>* is inactive, thereby inducing E93 expression. Wandering third-instar larvae (3LW) were dissected twenty-four hours later for immunostaining. (B) Box plots depicting quantification of E93 levels driven by *ci-GAL4* in 3LW wing discs relative to endogenous E93 levels in pupal wings 30h after puparium formation (APF) using anti-E93 antibodies. (C) Experimental details of the *vg-GAL4* lineage tracing experiments. Crosses were maintained at 29°C for thirty-six hours to permit *vg-GAL4* driven flip-out of the stop cassette. Crosses were then shifted to 18°C for 4.5 days. Finally, crosses were shifted back to 29°C for fifteen hours before dissecting wandering third-instar larvae (3LW). Due to the inefficiency of flip-out, some portion of each disc remains WT (white regions). (D) Box plots depicting quantification of E93 levels driven using the *vg-GAL4* system in 3LW wings relative to endogenous E93 in pupal wings 30hAPF using anti-E93 antibodies. Averages noted in red. n = 30 (10 measurements across 3 wings) per condition.



**Fig. S2. Additional examples of enhancer response to precocious E93.** (A, C, E) Precocious expression of E93 (magenta) in the anterior compartment using *ci-GAL4* deactivates the *br<sup>disc</sup>* enhancer, and activates the *tnc<sup>wv</sup>* and *tnc<sup>blade</sup>* enhancers (green). In control experiments lacking a 29°C shift (right panels), E93 was not expressed and no change in enhancer activity was observed. (B, D, F) Precocious expression of E93 (magenta) in the posterior compartment with *en-GAL4* deactivates the *br<sup>disc</sup>* enhancer and activates the *tnc<sup>blade</sup>* and *tnc<sup>wv</sup>* enhancers similarly to their response to E93 expression with *ci-GAL4*. (G) *tnc<sup>blade</sup>*

(green) is precociously activated by ectopic E93 expression in cells proximal to the outer ring of Wg (magenta). (H) Wild-type pMad pattern (yellow) in 3LW wing discs. Scale bars = 100µm.



**Fig. S3.** (A) Stacked bar chart plotting the fraction of total sites present at annotated genomic regions. Distributions are shown for the full set of E93 chip peaks, the mappable dm3 assembly, and each E93 binding category separately. (B) Average signal plot of FAIRE-seq signal within each binding category during wild-type 3LW and wild-type 24h APF wings. (C) Scatter plots of FAIRE signal (z-score) in wild-type 3LW and wild-type 24APF wings for each E93 binding category. Colors represent point density. Pearson's R values are reported for each category reflecting the correlation of FAIRE-seq z-scores between the two timepoints.

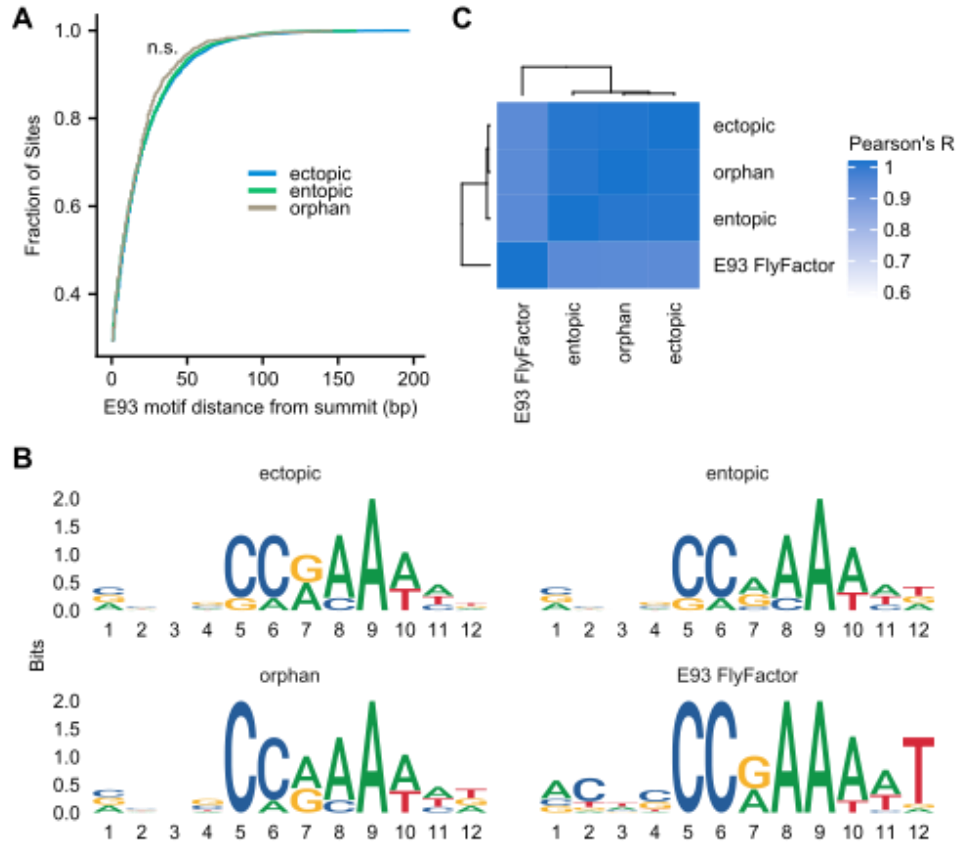


**Fig. S4.** (A) Cumulative distribution plot showing the distance from the summit to the nearest E93 motif. n.s. =  $p > 0.05$  KS-test. (B) PWMs derived from E93 motifs within E93 binding categories compared to the E93 motif from the Fly Factor Survey database. (C) Heatmap of Pearson correlation values between the PWMs shown in (B) values are hierarchically clustered.



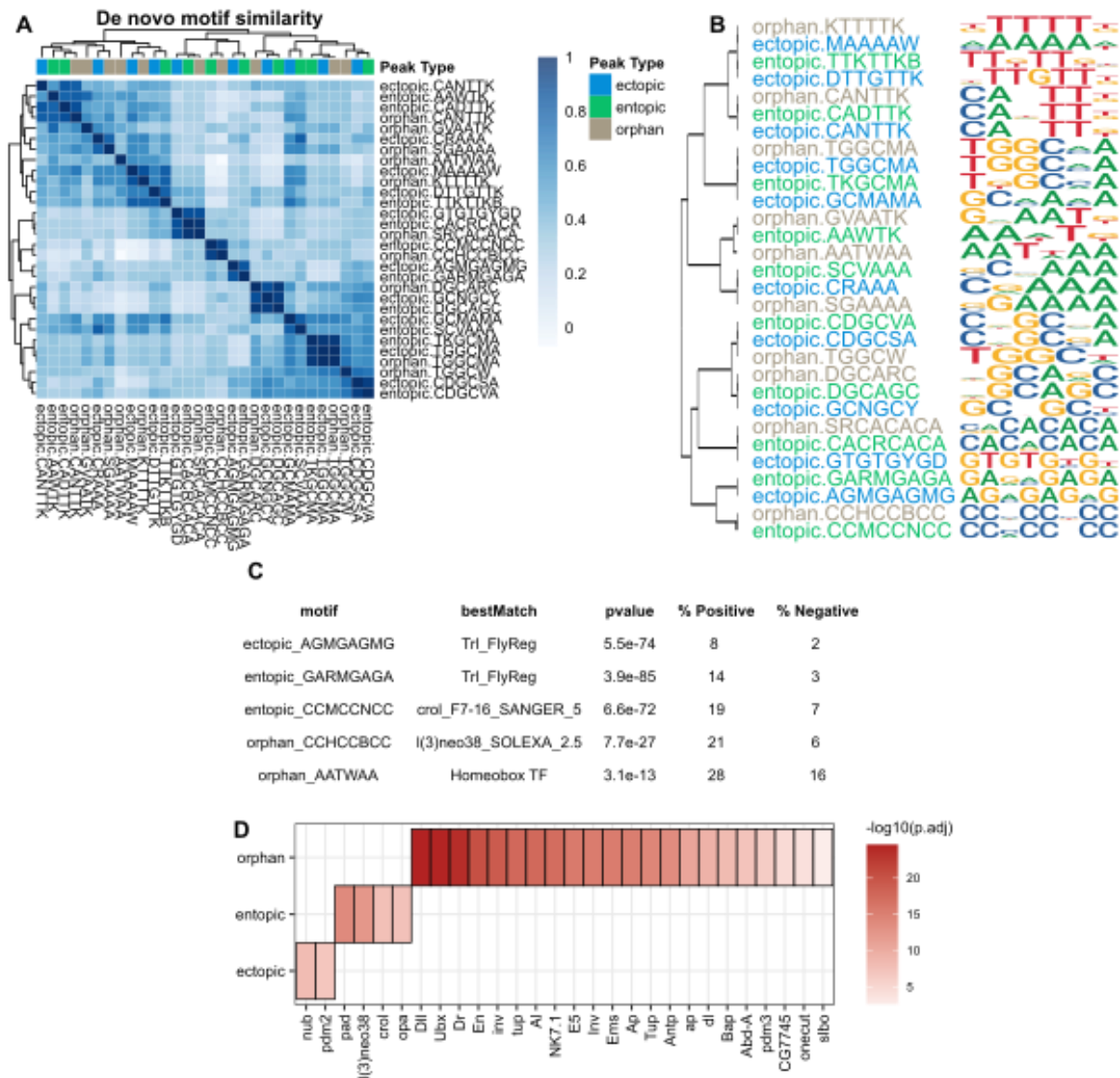


**Fig S5.** (A) Heatmap of PWM correlations for *de novo* discovered motifs within each E93 binding category. Color represents Pearson's R value. Heatmap is clustered by hierarchical clustering of correlation coefficients. (B) Clustering based on PWM distances. (C) Table displaying characteristics of *de novo* discovered motifs not found in all 3 binding categories. Best Match indicates the top matched Fly Factor Survey motif for the discovered PWM. Pvalue indicates the DREME p-value. % Positive and % Negative indicate the fraction of sites in foreground vs background sequences that contain a match to the *de novo* PWM. (D) Heatmap showing the top hits following directed motif scanning within each E93 binding category. Color represents  $-\log_{10}(\text{adjusted p-value})$  of enrichment.

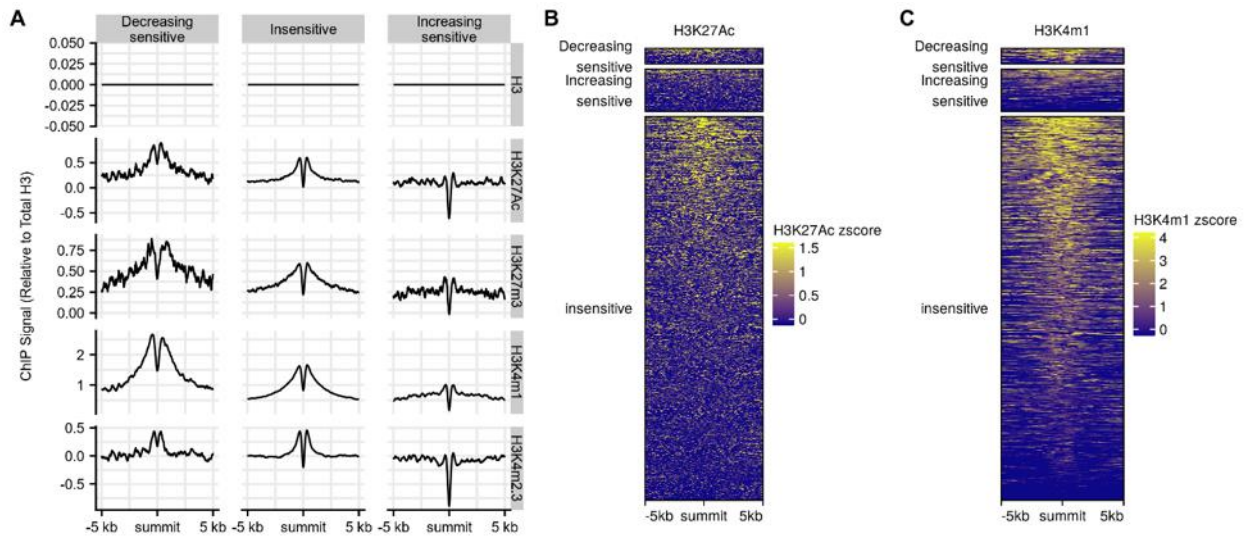


**Fig. S6.** (A) Average signal plots of histone PTM ChIP-seq z-scores (normalized to total H3 signal) at E93 sensitive and insensitive sites in wild-type 3LW wings. (B) Heatmap of H3K27Ac signal inside E93 sensitive sites. (C) Heatmap of H3K4m1 signal within E93 sensitive sites.

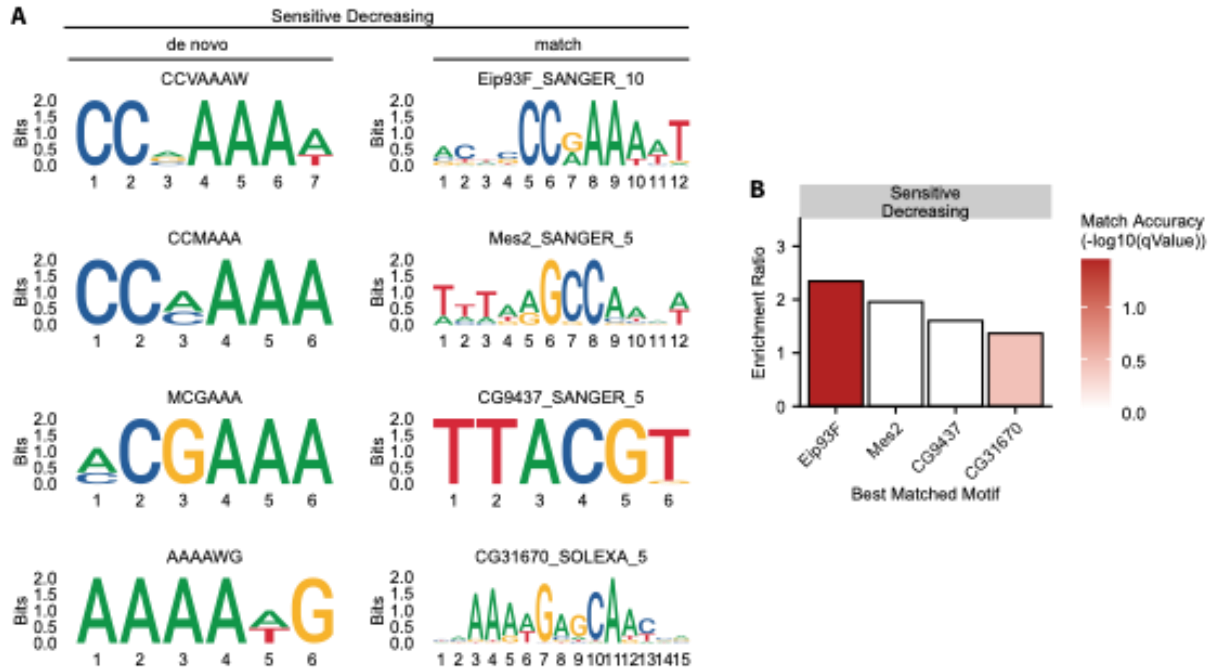


**Figure S7.** (A) PWMs of *de novo* discovered motifs within decreasing E93-sensitive sites compared to their corresponding best matched motif. The motif matching Mes2 strongly resembles the E93 motif. (B) Bar plot of enrichment ratio for *de novo* discovered motifs from (A) within E93 sensitive decreasing sites. Color of bar represents confidence that this PWM is the correct match to the *de novo* PWM.



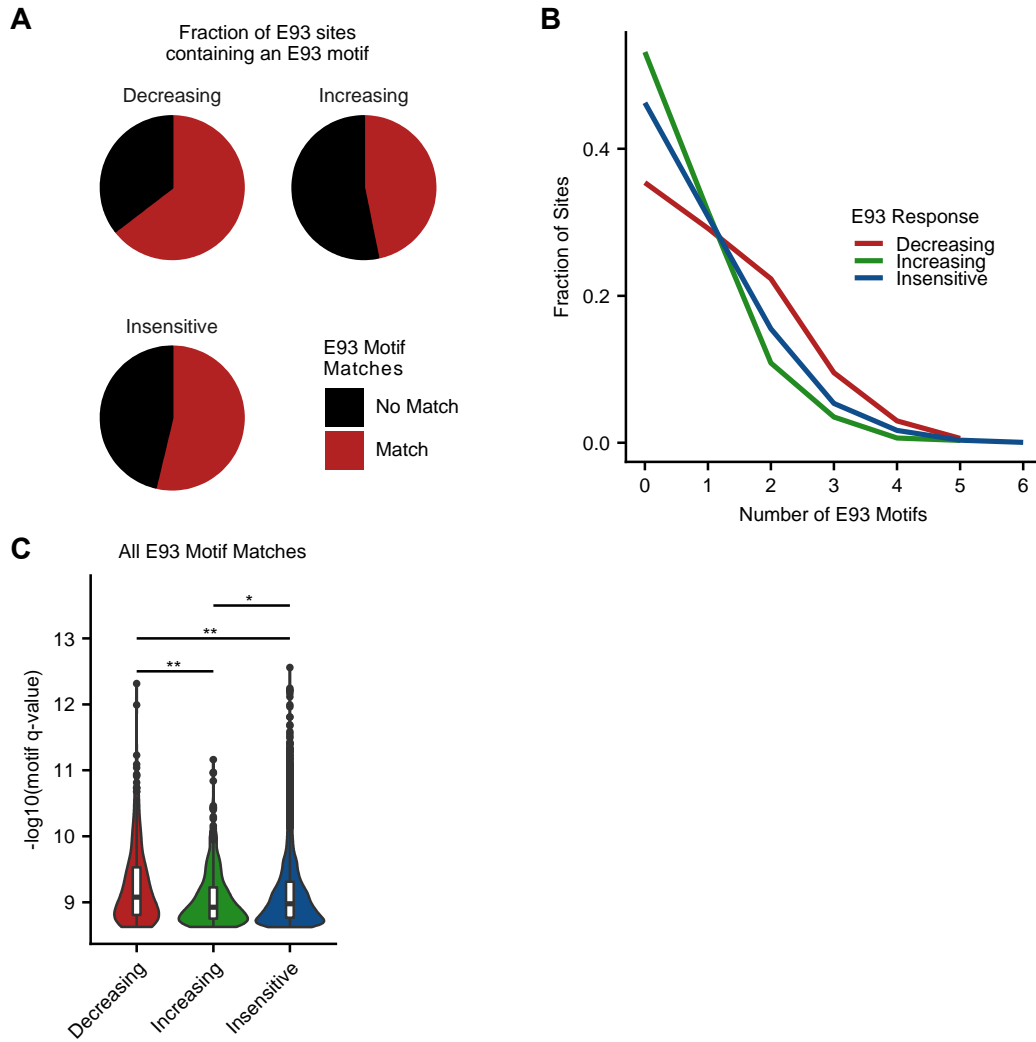


**Figure S8.** (A) Pie charts showing the fraction of E93 binding sites containing at least 1 match to the E93 motif. (B) Lineplot showing the fraction of E93 binding sites containing a given number of E93 motifs. (C) Violin plots depicting E93 motif quality within E93 binding sites. \* =  $p < 0.05$ , \*\* =  $p < 0.015$ , oneway anova followed by TukeyHSD test.

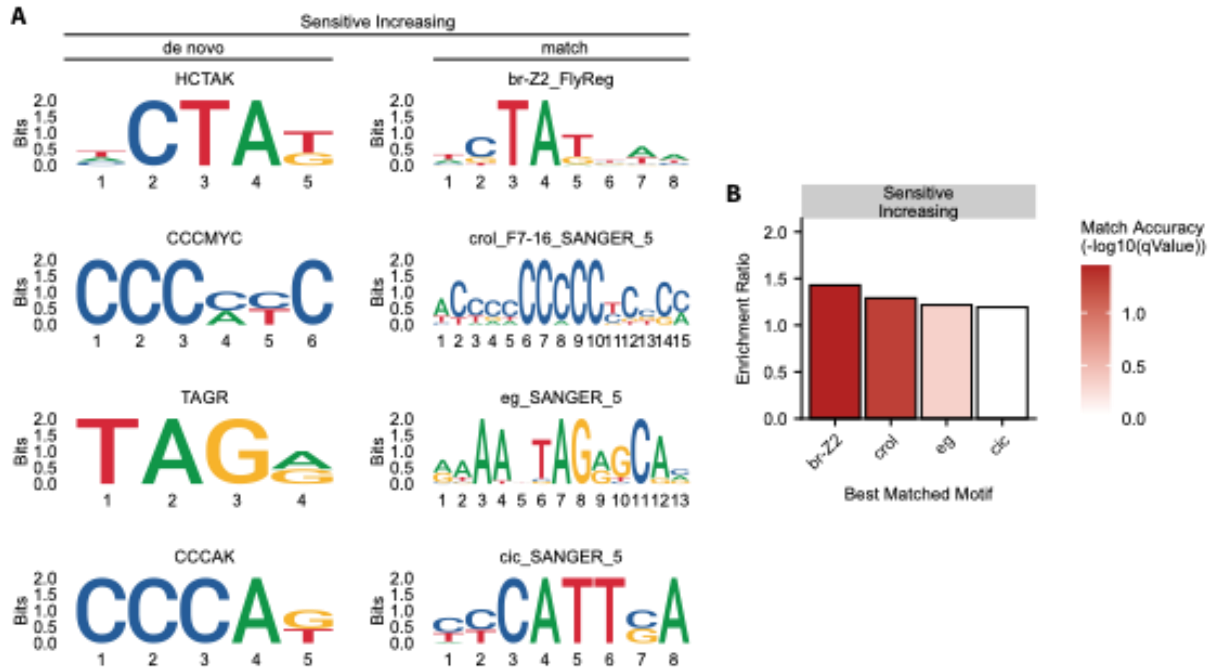


**Figure S9.** (A) PWMs of *de novo* discovered motifs within increasing E93-sensitive sites compared to their corresponding best matched motif. (B) Bar plot of enrichment ratio for *de novo* discovered motifs (from (A)) within increasing E93-sensitive sites. Color of bar represents confidence that this PWM is the correct match to the *de novo* PWM.

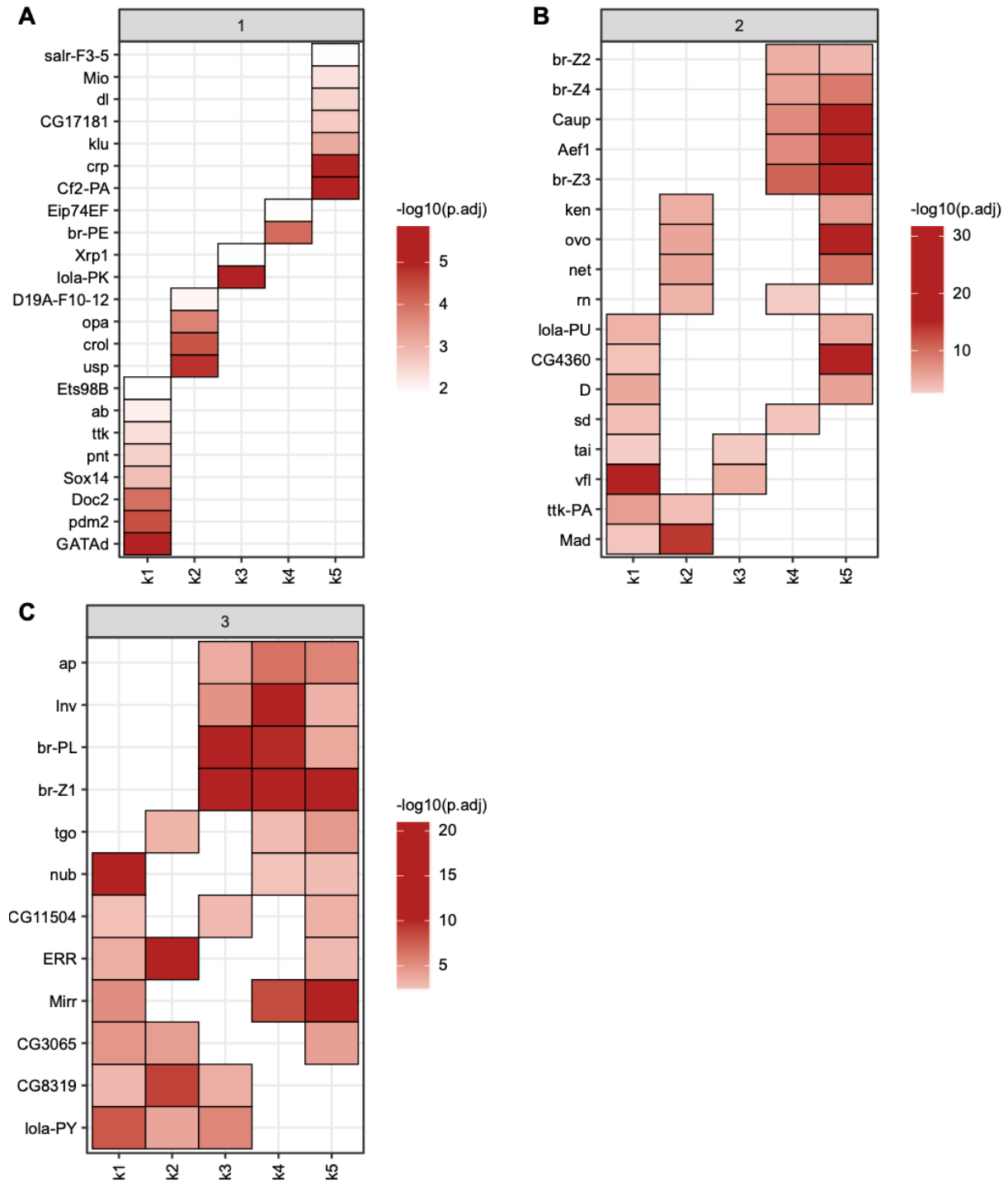


**Fig. S10.** Heatmaps of motifs detected in each temporal cluster. Facets represent motifs which are shared between 1, 2, or 3 clusters, (A–C) respectively. Color represents  $-\log_{10}(\text{adjusted p-value})$  of enrichment.



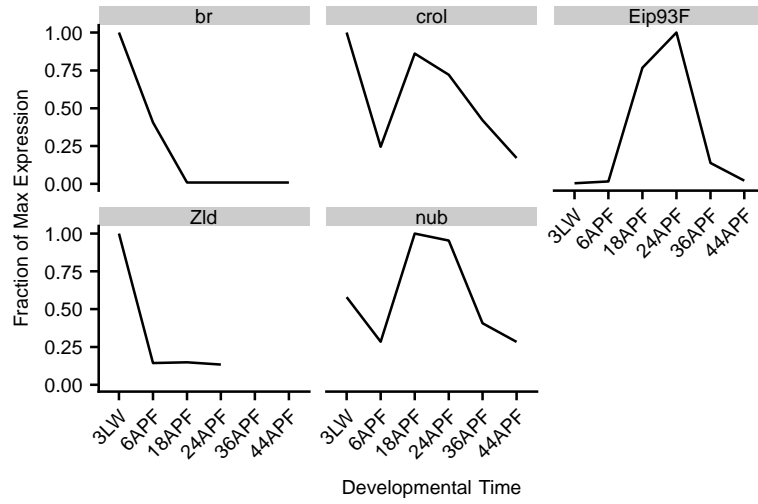


**Fig. S11.** mRNA levels of transcription factors identified in motif analyses plotted as the fraction of maximum signal during a wild-type wing developmental timecourse.